



Published in final edited form as:

Cancer Res. 2014 February 01; 74(3): 932–944. doi:10.1158/0008-5472.CAN-13-2474.

FANCI Localization by Mismatch Repair Is Vital to Maintain Genomic Integrity after UV Irradiation

Shawna Guillemette¹, Amy Branagan¹, Min Peng¹, Aashana Dhruva¹, Orlando D. Schärer², and Sharon B. Cantor¹

¹Department of Cancer Biology, University of Massachusetts Medical School, Women's Cancers Program, UMASS Memorial Cancer Center, Worcester, Massachusetts

²Department of Pharmacological Sciences & Department of Chemistry, Stony Brook University, Stony Brook, New York

Abstract

Nucleotide excision repair (NER) is critical for the repair of DNA lesions induced by UV radiation, but its contribution in replicating cells is less clear. Here, we show that dual incision by NER endonucleases, including XPF and XPG, promotes the S-phase accumulation of the BRCA1 and Fanconi anemia-associated DNA helicase FANCI to sites of UV-induced damage. FANCI promotes replication protein A phosphorylation and the arrest of DNA synthesis following UV irradiation. Interaction defective mutants of FANCI reveal that BRCA1 binding is not required for FANCI localization, whereas interaction with the mismatch repair (MMR) protein MLH1 is essential. Correspondingly, we find that FANCI, its direct interaction with MLH1, and the MMR protein MSH2 function in a common pathway in response to UV irradiation. FANCI-deficient cells are not sensitive to killing by UV irradiation, yet we find that DNA mutations are significantly enhanced. Thus, we considered that FANCI deficiency could be associated with skin cancer. Along these lines, in melanoma we found several somatic mutations in *FANCI*, some of which were previously identified in hereditary breast cancer and Fanconi anemia. Given that, mutations in *XPF* can also lead to Fanconi anemia, we propose collaborations between Fanconi anemia, NER, and MMR are necessary to initiate checkpoint activation in replicating human cells to limit genomic instability.

Corresponding Author: Sharon B. Cantor, Department of Cancer Biology, UMASS Medical School, 364 Plantation St., Worcester, MA 01605. Phone: 508-856-4421; Fax: 508-856-1310; Sharon.Cantor@umassmed.edu.

Disclosure of Potential Conflicts of Interest

No potential conflicts of interest were disclosed.

Authors' Contributions

Conception and design: S.B. Cantor

Development of methodology: S. Guillemette, M. Peng, S.B. Cantor

Acquisition of data (provided animals, acquired and managed patients, provided facilities, etc.): S. Guillemette, A. Branagan, O.D. Schärer

Analysis and interpretation of data (e.g., statistical analysis, biostatistics, computational analysis): S. Guillemette, A. Dhruva, S.B. Cantor

Writing, review, and/or revision of the manuscript: S. Guillemette, A. Branagan, O.D. Schärer, S.B. Cantor

Administrative, technical, or material support (i.e., reporting or organizing data, constructing databases): M. Peng, A. Dhruva, S.B. Cantor

Note: Supplementary data for this article are available at Cancer Research Online (<http://cancerres.aacrjournals.org/>).

Introduction

Repair of UV irradiation–induced DNA damage depends on the nucleotide excision repair (NER) pathway. Underscoring the essential role of NER in repair of UV-induced DNA damage, inherited defects in NER genes result in the skin cancer–prone disease xeroderma pigmentosum (1). In nonreplicating cells, NER factors sense UV-induced DNA damage and excise the lesion in a multistep process. The remaining short ssDNA region serves as a template for repair synthesis, “gap” repair (2, 3). Lesions escaping NER-dependent gap repair stall replication forks and initiate checkpoint responses. Some NER factors interact with the replisome and contribute to the early S-phase checkpoint response (4, 5). In postreplication, repair lesions are managed largely through DNA-damage tolerance mechanisms (6-8). Among the recent factors found to be involved in this process is the hereditary breast cancer–associated gene product BRCA1, which function independently of NER to suppress mutations (9).

Several lines of evidence indicate that UV-induced damage is also limited by proteins of the DNA mismatch repair (MMR) pathway. MMR factors induce checkpoints, apoptosis, preserve genomic stability, and suppress cancer induced by UV irradiation (10-14). The mechanism by which MMR functions in response to UV irradiation could stem from its general role in genome surveillance and mismatch correction. Canonical MMR begins with the recognition of replication errors (15), where MSH2–MSH6 (MutS α) or MSH2–MSH3 (MutS β) assemble and recruit the heterodimer MLH1–PMS2 (MutL α). These complexes function in the repair of mismatched bases. As such, loss of MMR confers a mutator phenotype and a predisposition to hereditary nonpolyposis colon cancer (HNPCC; ref. 16). However, it is also well appreciated that MMR proteins respond to DNA damage from exogenous sources, such as to DNA alkylating agents, known to induce mismatches following DNA replication (17). In response to UV irradiation, MMR factors could have an alternative noncanonical role in UV lesion processing given that the MSH2–MSH6 complex directly binds UV lesions (18, 19). Clarifying how MMR contributes to genomic stability in the UV response will be central to understanding the HNPCC variant, Muir–Torre syndrome that is characterized by skin cancers (20-22).

Both the MMR protein MLH1 and BRCA1 bind directly to the DNA helicase FANCD1, which has essential functions in activating checkpoints following replication stress, although it has not hitherto been linked to the UV-induced damage response (23-27). FANCD1 is mutated in hereditary breast and ovarian cancer as well as in the rare cancer-prone syndrome Fanconi anemia (24, 28). Complementation studies using FANCD1-deficient (FA-J) patient cells demonstrated that MLH1 binding is critical for FANCD1 function in the repair of DNA interstrand crosslinks (24, 29). Here, we reveal that MLH1 binding to FANCD1 is also essential for the response to UV-induced damage, in which FANCD1 promotes an S-phase checkpoint point and limits UV-induced mutations. Because dual incision by NER also promotes FANCD1 accumulation at sites of UV-induced damage, and the NER endonuclease XPF was recently shown to be a Fanconi anemia gene (30, 31), our analysis suggests that Fanconi anemia, MMR, and NER pathways collaborate to process UV lesions in S-phase cells to preserve the genome.

Materials and Methods

Cell culture

A549, MCF7, and U2OS cells were cultured in Dulbecco's Modified Eagle Medium (DMEM; Gibco; Life Technologies) supplemented with 10% FBS and 1% penicillin/streptomycin. *FA-J*, 48BR, MEFs, GM04429 *XP-A*, XP2YO *XP-F*, and XPCS1RO *XP-G* cells, and their respective complements were cultured in DMEM supplemented with 15% FBS and 1% penicillin/streptomycin. Patient cell lines XP2YO *XP-F*, XPCS1RO *XP-G*, and their respective complements were generated by Dr. O. Schärer and MSH2^{-/-} or MSH2^{+/-} MEFs were a generous gift of J. Stavnezer.

DNA constructs

FA-J cells were infected with pOZ retroviral vectors (32), expressing FANCI^{WT}, FANCI^{K141/142A}, FANCI^{S990A}, or empty vector as described earlier (23, 24). Stable cell lines were generated by sorting with anti-IL-2 magnetic beads (Dyna Beads). The pCDNA-3myc-6xhis vectors were generated with a QuickChange Site-Directed Mutagenesis Kit (Stratagene) using published primers for FANCI^{K52R} (23). GFP-polh was expressed in U2OS cells as described in refs. 28, 33, and 34.

RNA interference

The packaging cell line 293TL was used to produce lentiviral particles containing pGIPZ or pLKO.1 vectors and 293TD cells were used to produce retroviral particles containing pStuffer vector. Cells were transfected with 1:1:2 µg of DNA packaging versus insert using Effectene Transfection Reagent (Qiagen) 48 hours before harvesting retroviral or lentiviral supernatants. Supernatants were filtered and added to recipient cell lines with 1 µg/mL polybrene. Cells infected with short hairpin RNA (shRNA) vectors were selected with either puromycin (pGIPZ, pLKO.1) or hygromycin (pStuffer). For shRNA-mediated silencing, the mature antisense was used for pLKO.1 shNSC 5'-CCGCAGGTATGCACGCGT-3', shMLH1 5'-AATACAGAGAAAGAACAACAC-3', shMSH2 5'-AAACTGAGAGAGATTGCCAGG-3', shXPF 5'-AAATCACTGATACTCTTGCGC-3', shFANCI 5'-TATGGATGCCTGTTTCTTAGCT-3', for pGIPZ shNSC 5'-ATCTCGCTTGGGCGAGAGTAAG-3', shMSH2-1 5'-ATTACTTCAGCTTTTAGCT-3', shMSH2-2 5'-GCATGTAATAGAGTGTGCTAA-3', shMSH6-1 TTCAACTCGTATTCTTCTGGC, and shMSH6-2 TTTCAACTCGTATTCTTCTGG. The pStuffer vectors were a generous gift of Dr. J. Chen. The pStuffer shRNA-targeting luciferase was 5'-GUGCGCUGCUGGUGCCAAC-3', shFANCI-1 5'-GUACAGUACCCACCUUAU-3', and shFANCI-2 5'-GAUUUCCAGAUCACAAUU-3'. RNAi-mediated depletion of Luciferase, FANCI, or RAD18 using siRNA reagents was performed as described previously (28).

Local UV irradiation and immunofluorescence

Local UV irradiation was performed as described (35) using a 254 nm UV lamp (UVP Inc.) with a dose of 100 J/m², although 3- or 5-µm Isopore polycarbonate membrane filters (Millipore). Cells were fixed for 10 minutes with either ice cold methanol or 3%

paraformaldehyde/2% sucrose in PBS, permeabilized for 5 minutes with 0.5% Triton X-100, and treated with 0.08M NaOH for 2 minutes only before using 6-4 pyrimidine-pyrimidone (6-4 PP) or cyclobutane pyrimidine dimer (CPD) Abs. Coverslips were rinsed 3× in 1× PBS before each step. For primary and secondary staining, cells were incubated for 40 minutes each in a humid chamber, face down on a 100 μL meniscus of Abs diluted in 3% bovine serum albumin (BSA) in PBS. Primary Abs used were anti-FANCI (1:500; Sigma; Lot #051M4759, #014K4843), anti-phospho-S4/S8 RPA32 (1:500; Bethyl), anti-MLH1 (1:200; BD Bioscience), anti-MSH2 (1:200; Calbiochem), anti-XPF (1:200; Neomarkers), anti-ERCC1 (1:500; Santa Cruz), anti-XPC (1:500; Abcam), anti-6-4 PP, and anti-CPD (both 1:1,000; CosmoBio). Secondary Abs used include Rhodamine Red-X–conjugated AffiniPure Goat anti-rabbit or anti-mouse immunoglobulin G (IgG) and fluorescein (FITC)-conjugated AffiniPure Goat anti-rabbit IgG (Jackson Immuno-Research Laboratories Inc.). Coverslips were mounted on slides using Vectashield mounting media with 4',6-diamidino-2-phenylindole (DAPI; Vecta laboratories, Inc.) and analyzed on a fluorescence microscope (Leica DM 5500B) with a Qimaging Retiga 2000R Fast 1394 camera. For each experimental time point, 400 DAPI-positive cells (1,200 in triplicate) were analyzed using Q-Capture Pro line intensity profile software with the intensity gated at 0.1 for positive localized UV damages (LUD) for 6-4 PP or CPD staining. The accumulation of a protein at an LUD was considered positive if its intensity was 10-fold greater than the line drawn over the rest of the nucleus.

Mutation frequency assays

The hypoxanthine phosphoribosyltransferase (HPRT) assay was performed in A549 cells as described (36) with the following modifications. After culturing cells for 1 week in media containing hypoxanthine, aminopterin, and thymidine (HAT selection) to eliminate background *HPRT* mutations, cells were stably depleted of FANCI with 2 unique shRNA targets versus a nonsilencing control (NSC) and selected with hygromycin. UV-induced HPRT mutants were obtained by seeding 6 plates at a confluence of 1×10^6 cells/10-cm dish 24 hours before either mock treatment, 5, or 10 J/m² UV irradiation in a 254-nm Spectrolinker XL-1500 (Dot Scientific, Inc.). Posttreatment cells were allowed to recover to 6×10^6 cells or with mock cells 6 population doublings and 6×10^6 cells were seeded at a confluence of 1×10^6 /10-cm dish in media containing 24 μM 6-thioguanine (6-TG) to select for HPRT-inactivated colonies. At the same time, 200 cells were also seeded in 6-TG-free media to determine colony-forming efficiency. The frequency of inactivating mutations at the *HPRT* locus was calculated as the [(no. of total 6-TG-resistant colonies)/(6×10^6 cells seeded)] × the colony-forming efficiency. HPRT inactivation frequency represents the mean of 3 independent experiments. Individual colonies were picked and grown until enough cells were obtained for RNA isolation using TRizol reagent (Life Technologies) according to the manufacturer's protocol. The HPRT gene was subjected to reverse transcription-PCR using SuperScript (Invitrogen) followed by sequencing using overlapping primers HPRT1 5'-CTTCTCCTCCTGAGCAGTC-3', HPRT2 5'-AAGCAGATGGC-CACAGAACT-3', HPRT3 5'-CCTGGCGTCGTGATTAGTG-3', HPRT4 5'-TTTAC-zTGGCGATGTCAATAGGA-3', HPRT5 5'-GACCAGTCAACAGGGGACAT-3', and HPRT6 5'-ATGTCCCCTGTTGACTGGTC-3'. Patient-derived *FA-J* cells were complemented with empty vector or FANCI^{WT} and treated as described with A549 cells. As

FA-J cells do not make colonies, the % increase in 10 $\mu\text{mol/L}$ 6-TG survival was calculated as the % of UV-irradiated cells surviving 6-TG minus the % of untreated cells surviving 6-TG. The % increase in 6-TG survival represents the mean of 3 independent experiments.

EdU labeling

EdU incorporation was performed as described previously (37), except cells were seeded on coverslips and left untreated or UV-irradiated through 5- μm filters before 3-hour incubation in 10 $\mu\text{mol/L}$ EdU diluted in serum-free media. When using global UV irradiation, cells were left untreated and pulsed 45 minutes in 10 $\mu\text{mol/L}$ EdU or UV irradiated and pulsed 16 hours later for 45 minutes with 10 $\mu\text{mol/L}$ EdU. Cells were processed by Click-iT EdU Imaging Kit (Invitrogen) using the manufacturer's instructions immediately followed by the above immunofluorescence protocol.

Western blot analysis

Cells were harvested and lysed in 150 mmol/L NETN (0.5% NP-40 detergent, 1 mmol/L EDTA, 20 mmol/L TRIS, 150 mmol/L NaCl) lysis buffer [20 mmol/L Tris (pH 8.0), 150 mmol/L NaCl, 1 mmol/L EDTA, 0.5% NP-40, 1 mmol/L phenylmethylsulfonyl fluoride, and 1 \times protease inhibitor cocktail] for 30 minutes on ice. Cell extracts were clarified by centrifugation at 14,000 rpm, protein was quantified by Bradford assay, and lysates were boiled in SDS-loading buffer. Chromatin extracts were prepared as described (38). For CPD immunoprecipitation, cells were lysed in 150 mmol/L NETN buffer, spun down, and the insoluble pellet was resuspended in radioimmunoprecipitation assay buffer (RIPA) and sonicated. The RIPA fraction was spun down and chromatin lysate was quantified by Bradford assay. Lysates were then precleared with Protein A beads and immunoprecipitated overnight with CPD Abs. Proteins were separated by SDS-PAGE on 4% to 12% bis Tris or 3% to 8% Tris Acetate gels (Novex; Life Technologies) and electrotransferred onto nitrocellulose membranes. Membranes were blocked in 5% milk diluted in PBS. Antibodies used for Western blot analysis included anti-FANCI [1:1,000; Sigma, 1:1,000; E67 (previously described; ref. 39)], anti-Bactin (1:5,000; Sigma), anti-MLH1 (1:500; BD Bioscience), anti-MSH2 (1:500; Calbiochem), anti-MSH2 (mouse specific; Santa Cruz), anti-XPF (1:1,000; Neomarkers), anti-ERCC1 (1:500; Santa Cruz), anti-XPC (1:1,000; Abcam), anti-CHK1 (1:500; Bethyl), anti-p317 CHK1 (1:500; Bethyl), anti-RPA32 (1:500; Bethyl), and anti-phospho-S4/S8 RPA32 (1:500; Bethyl). Membranes were washed and incubated with horseradish peroxidase-linked secondary antibodies (Amersham; 1:5,000), and detected by chemiluminescence (Amersham). The ratio of phospho-protein to total protein was measured and quantified using Image J software.

Fluorescence-activated cell sorting analysis

FA-J cells cultured to ~80% confluency were left untreated or globally irradiated with 5 J/m^2 before collecting and fixing in 70% ethanol 4 hours after UV irradiation. For antibody labeling, cells were rinsed with 1 \times PBS, permeabilized with 0.5% Triton-X 100 in PBS 20 minutes at room temperature, and then washed with 1% BSA/0.25% Tween-20 in PBS (PBS-TB) before resuspending 1 hour in PBS-TB with phospho-S4/S8 replication protein A (RPA) 32 antibody (1:250; Bethyl). Cells were then collected and washed 2 \times in PBS-TB before 1-hour incubation in PBS-TB containing FITC-conjugated AffiniPure Goat Anti-

Rabbit IgG (1:200; Jackson Immuno-Research Laboratories, Inc.). After washing with PBS, cells were resuspended in RNase A solution (100 µg/mL in PBS) for 20 minutes at room temperature and again washed with PBS before fluorescence-activated cell sorting (FACS) analysis. Cells were labeled with propidium iodide before analysis on a FACSCaliber flow cytometer (Becton-Dickinson) performed at the University of Massachusetts Medical School flow cytometry core facility using Cellquest software. The fluorescence intensity of phospho-S4/S8 RPA 32-positive cells was gated as FITC-positive cell populations compared with no antibody control.

Results

FANCI accumulation at sites of UV-induced damage is dependent on NER dual incision

We examined the response of FANCI to UV irradiation by assessing whether FANCI accumulated at sites of UV-induced damage. Following UV irradiation through 3 or 5 µm filters to generate sites of LUDs (35, 40), we found that FANCI colocalized with UV-induced 6-4 PPs, CPDs, and the NER endonuclease XPF in the breast cancer cell line, MCF7. FANCI localization to 6-4 PP- or XPF-positive LUDs peaked ~3 hours after UV irradiation and diminished by ~12 hours (Fig. 1A and B).

To address the relationship of FANCI to NER, we used *XP* fibroblast cell lines and their functionally complemented counterparts. We found that the accumulation of FANCI at LUDs was reduced ~2- to 3-fold in NER-deficient *XP-A*, *XP-F*, and *XP-G* cells when compared with the wild-type complemented cells (Fig. 1C-F). Contributing to FANCI localization was XPF and XPG endonuclease activity as complementation with XPF or XPG nuclease-defective mutant species, XPF^{D676A} or XPG^{E791A} (41) failed to restore robust FANCI accumulation at LUDs between ~1 and 5 hours after UV-induced damage (Fig. 1E and F). Following global UV irradiation, FANCI foci were also more prominent in *XP-F* cells complemented with wild-type XPF endonuclease (Supplementary Fig. S1A and S1B). By contrast, FANCI depletion did not affect the localization dynamics of NER factors (Supplementary Fig. S1C and S1D). Collectively, these data indicate that NER incision events potentiate the accumulation of FANCI to sites of UV-induced damage.

NER promotes the accumulation of FANCI at UV-induced damage in S phase

Next, we investigated whether NER contributed to FANCI accumulation at LUDs in a specific cell-cycle phase. Cells within S phase and non-S phase can be easily distinguished after local UV irradiation by staining for 5-ethynyl-2'-deoxyuridine (EdU) incorporation into genomic DNA (37). In S-phase cells, EdU staining is bright and pan nuclear. In non-S-phase cells, EdU staining is restricted to sites of LUDs, representing sites of unscheduled DNA synthesis that occurs during gap repair in NER (42). Following localized UV irradiation, cells were incubated in media with EdU for 3 hours and immunostained with FANCI antibodies. Consistent with a role for XPF in NER-dependent gap filling, EdU-positive LUDs in non-S-phase cells were only present in XPF^{WT} cells (Fig. 1G and H). FANCI recruitment to LUDs was not significantly improved in non-S-phase XPF^{WT} cells, however it was significantly enhanced in S-phase XPF^{WT} cells, indicating that XPF potentiates FANCI accumulation in cells undergoing DNA synthesis (Fig. 1G and H).

FANCI localization to sites of UV-induced damage is MMR dependent

FANCI directly binds BRCA1, which functions in the response to UV irradiation selectively in S-G₂ phase cells (9, 23). FANCI also directly binds MLH1 (24), which along with other MMR factors function in the response to UV irradiation and preserve genomic integrity (43). Because both BRCA1 and MLH1 contribute to FANCI localization and function in the DNA-damage response (24, 28, 29, 44), we investigated whether BRCA1 or MLH1 interactions were required for FANCI localization to LUDs. We analyzed FANCI recruitment in FANCI-deficient *FA-J* patient cells complemented with empty vector, FANCI^{WT}, the BRCA1-interaction defective mutant (FANCI^{S990A}; ref. 45), or the MLH1-interaction defective mutant (FANCI^{K141/142A}; ref. 24). Although the FANCI species expressed at similar levels, we found that FANCI^{K141/142A} localization was dramatically reduced as compared with FANCI^{S990A}, which localized to LUDs just as efficiently as FANCI^{WT} (Fig. 2A–C). Importantly, FANCI-positive LUDs were not detected in FANCI-null *FA-J* cells unless complemented with wild-type FANCI, confirming the specificity of our FANCI antibody (Fig. 2A–C). Further validating that FANCI localization to LUDs requires functional MMR, we found that as compared with a NSC, FANCI recruitment to LUDs was severely reduced in U2OS cells depleted of MLH1, MSH2, or MSH6 (Fig. 2D–I and Supplementary Fig. S2A and S2D). In contrast, XPC and ERCC1 recruitment to LUDs was not affected by MSH2 depletion (Supplementary Fig. S2E and S2F), indicating that MMR is required for accumulation of FANCI at LUDs, but not XPC or ERCC1. Similarly, MSH2 recruitment to LUDs was similar in vector and XPF^{WT} complemented *XP-F* cells whereas as expected ERCC1 was only present in the XPF^{WT} complemented *XP-F* cells, suggesting that MMR and NER accumulation at LUDs is not inter-dependent (Supplementary Fig. S2G and S2H). We also noted that the residual accumulation of FANCI found at LUDs in *XP-F* cells was eliminated by depletion of MSH2 (Fig. 2J–L), suggesting that NER and MMR operate in a parallel manner to support FANCI localization. In the *XP-F* cells, however MSH2 depletion did not perturb FANCI nuclear or chromatin localization, suggesting MMR and NER contribute to FANCI localization to LUDs as opposed to nuclear import (Supplementary Fig. S2I).

We expected that both NER and MMR would also be present in S-phase cells given that they contribute to the S-phase localization of FANCI. However, NER proteins are best known for their UV repair function in non-S-phase cells (3) and from the literature it was not clear if MMR proteins had a cell-cycle-dependent localization to LUDs. We used primary immortalized 48BR fibroblasts that have been used to characterize NER proteins in gap repair by means of EdU incorporation (42). Although XPF was clearly present in non-S-phase cells at sites of gap filling, as expected, we also detected XPF in nearly all LUDs in S-phase cells, ~95% (Supplementary Fig. S3A–S3C). MLH1 and MSH2 were also present at LUDs with a similar percent in both non-S- and S-phase cells. Instead, FANCI was primarily at LUDs in S-phase cells, ~86% and only in ~19% of non-S-phase cells (Supplementary Fig. S3A–S3C). Collectively, these studies show that MMR and NER proteins localize to LUDs in both non-S- and S-phase cells, whereas FANCI localizes primarily in S-phase cells.

FANCI promotes the UV-induced arrest of DNA synthesis and the induction of RPA phosphorylation

UV irradiation activates checkpoint responses and inhibits DNA replication in S-phase cells (46). Given the role of FANCI in checkpoint responses (25-27) and the accumulation of FANCI at LUDs during S phase, we tested if FANCI contributed to the UV-induced checkpoint response. By pulsing cells with EdU, we found that *FA-J* cells expressing FANCI^{WT} underwent a 10.5-fold reduction in S-phase cells when examined 16 hours after UV irradiation. By comparison, *FA-J* cells expressing vector underwent a 2.0-fold reduction (Fig. 3A and B), indicating that FANCI contributes to the arrest of DNA synthesis in response to global UV irradiation.

The UV-induced arrest of DNA synthesis is also associated with changes in phosphorylation of the ssDNA binding protein RPA (47). Following UV irradiation, the 32 kDa subunit of RPA is phosphorylated on several serine residues in the N-terminal of the protein in a cell-cycle-dependent manner by DNA-PK and cyclin-dependent kinases (48, 49). By examining phosphorylation of serines4/8 on RPA32 with a specific antibody, we found that in response to global UV irradiation, FANCI complementation was sufficient to enhance RPA serines4/8 phosphorylation in *FA-J* cells by FACS (Fig. 3C) and immunoblot (Supplementary Fig. S3D) analyses. By FACS analysis, basal phospho-S4/8 RPA32 was ~1% to 2% in both untreated vector and wild-type FANCI complemented *FA-J* cells. Following UV irradiation, phospho-S4/8 RPA32 was induced to ~22% in FANCI^{WT} *FA-J* cells as compared with only ~7% in vector *FA-J* cells (Fig. 3C). Similarly, using phospho-S4/8 RPA32 immunostaining in conjunction with EdU pulse, we uncovered that phospho-S4/8 RPA32 staining was detected only in S-phase cells (Fig. 3D and E). Furthermore, we found that *FA-J* patient cells complemented with FANCI^{WT} or the BRCA1-interaction defective mutant (FANCI^{S990A}) had significantly greater EdU-positive S-phase cells with phospho-S4/8 RPA32-positive LUDs as compared with the *FA-J* cells complemented with empty vector or the MLH1-interaction defective mutant (FANCI^{K141/142A}; Fig. 3D and E). This finding further suggested that FANCI and the FANCI-MLH1 interaction, but not the BRCA1 interaction, contributes to checkpoint responses in S-phase cells.

Immunoblotting in FANCI-depleted MCF7 cells also revealed that phospho-S4/8 RPA32 as well as the soluble checkpoint factor phospho-317 CHK1 was reduced compared with NSC whereas total CHK1 and RPA levels were unchanged (Fig. 3F and G). Moreover, co-immunostaining with phospho-S4/8 RPA32 and 6-4 PP antibody was used to visually mark UV-induced LUDs and revealed that phospho-S4/8 RPA32 was significantly reduced in FANCI-depleted cells as compared with NSC (Fig. 3H-J). Interestingly, by 12 hours post-UV damage, 6-4 PP LUDs persisted in FANCI-depleted cells (Fig. 3H-J). FANCI or MSH2 depletion also consistently enhanced the persistence of 6-4 PP-positive LUDs in the male lung cancer cell line, A549 in which the formation of phospho-S4/8 RPA32-positive LUDs was also significantly reduced (Supplementary Fig. S4A-S4C). Furthermore, the combination of FANCI and MSH2 depletion was not additive (Supplementary Fig. S4A-S4C), suggesting that FANCI and MSH2 function in a common pathway that is not cell-type specific.

Recently, NER factors were shown to promote the S-phase checkpoint response, including RPA phosphorylation in response to UV irradiation (4, 5, 50). Given that the mechanism by which NER promotes the S-phase checkpoint is unclear, we considered whether the NER-dependent accumulation of FANCI at LUDs in S phase was required. As before, *XP-F* patient cells were segregated into non-S- and S-phase cells by labeling with EdU and phospho-S4/8 RPA32 staining was detected only in S-phase cells (Fig. 4A and B). We found that phospho-S4/8 RPA32 induction was greatest in *XP-F* cells complemented with XPF^{WT} (Fig. 4A–C). Strikingly, depletion of FANCI or MSH2 profoundly reduced the phospho-S4/8 RPA32 induction of XPF^{WT} complemented *XP-F* cells (Fig. 4A–E). Notably, the residual phospho-S4/8 RPA32-positive LUDs found in vector complemented *XP-F* cells were also reduced by depletion of FANCI or MSH2 (Fig. 4A–E). Thus, FANCI promotes S-phase checkpoint responses in not only cancer cell lines, but also in nontransformed fibroblasts. Together, these data suggest that MSH2 and FANCI contribute to NER-dependent and -independent UV-induced phospho-S4/8 RPA32 induction at LUDs in S-phase cells. In contrast, when either FANCI or MSH2 were depleted, we found gap filling was proficient in the *XP-F* cells complemented with XPF^{WT} (Fig. 4A and B and E–H). Gap filling was also proficient in 48BR cells depleted of FANCI, MLH1, or MSH2, but reduced in cells depleted of XPF (Supplementary Fig. S4D). *Msh2*^{-/-} and *Msh2*^{+/+} mouse embryonic fibroblasts also had similar levels of gap filling (Supplementary Fig. S4E), suggesting that FANCI and MMR factors are not required for NER-dependent gap filling.

Collectively, our data indicate that FANCI contributes to the UV-induced arrest of DNA synthesis by potentiating checkpoint induction pathways. Although FANCI does not contribute to NER-dependent gap repair, it influences the clearance of UV-induced lesions in a common pathway with MSH2.

FANCI suppresses UV-induced mutations

Given that FANCI is dispensable for survival after UV exposure (28), we sought to examine if FANCI preserves the integrity of the genome, as has been found for MMR (14). A549 cells are useful for analyzing mutations at the endogenous *HPRT* locus (36). Similar to other cell lines examined, in A549 cells FANCI localized to sites of UV-induced damage as demonstrated by co-precipitation of FANCI with CPD and modified proliferating cell nuclear antigen (PCNA) following UV-induced damage (Supplementary Fig. S5A). Using RNAi-mediated FANCI silencing, we confirmed that FANCI was not essential for survival following UV irradiation, but was essential for survival following exposure to the DNA cross-linking agent cisplatin (Fig. 5A–C and Supplementary Fig. S6A and S6B). As compared with NSC, we found that FANCI depletion enhanced UV-induced *HPRT*, inactivating mutations determined by clonal selection in 6-TG (36). FANCI depletion did not affect spontaneous *HPRT* mutations, but the frequency of inactivating *HPRT* mutations after 10 J/m² UV irradiation was enhanced ~10-fold in A549 cells (Fig. 5D). Sequencing of clones arising from *HPRT* inactivation indicated no gross deletions or rearrangements as a consequence of FANCI deficiency in response to global UV irradiation. Instead, *HPRT* inactivation was predominated by ~8-fold more C to T transitions in both the transcribed strand and nontranscribed strand (NTS) of *HPRT* in FANCI-depleted cells (Fig. 5E and F and Supplementary Table S1). These findings suggest that FANCI is involved in a specific

process that suppresses the formation of point mutations in response to UV irradiation. Further supporting that FANCI suppresses inactivating mutations at the *HPRT* locus, FANCI^{WT} complementation in FANCI-deficient FA-J patient cells was sufficient to reduce survival in 6-TG after UV irradiation, indicating that FANCI averted the occurrence of mutations (Supplementary Fig. S6C). Furthermore, complementation with FANCI^{WT} enhanced resistance to DNA cross-linking agent, mitomycin C, although in accordance with the results from Fig. 4C, the resistance to UV irradiation was unchanged (Supplementary Fig. S6D and S6E). Together, these results suggest that FANCI, similar to MMR (10-14), contributes to the prevention of mutations in response to UV irradiation, without affecting long-term survival following this treatment. Thus, we propose that in collaboration with NER, the MMR-FANCI pathway is important for the response to UV irradiation in S phase to ensure checkpoint responses, genome stability, and limit tumorigenesis (Fig. 5G).

Discussion

Here, we show that both NER and MMR proteins promote the localization of the FANCI DNA helicase to sites of UV-induced lesions to ensure a robust S-phase checkpoint response. MMR proteins initially recruit FANCI and its further accumulation requires dual incision by the NER endonucleases XPF and XPG (Figs. 1C–H and 2D–L). Although FANCI deficiency does not cause UV-induced sensitivity, our analysis revealed an important role for FANCI in promoting an S-phase checkpoint response, lesion repair, and suppressing UV-induced mutations (Figs. 3A–J, 4A–E and 5A–F and Supplementary Figs. S3D, S4A–S4C, and S6C). Consistent with FANCI and MMR functioning in a common pathway, we found that FANCI or MMR deficiency alone or in combination generated similar defects (Supplementary Fig. S4A–S4C). Correspondingly, the direct interaction between MLH1 and FANCI is essential for both FANCI localization and function at sites of UV-induced damage, whereas the BRCA1 interaction is not required (Figs. 2A–C and 3E and F). Similar to NER, MMR proteins localize to LUDs in both non-S- and S-phase cells, whereas FANCI is predominantly found at sites of UV-damage in S-phase cells (Supplementary Fig. S3A–S3C). Together, our work demonstrates that distinct pathways merge in S-phase cells to ensure a robust UV-induced DNA damage response.

These findings are important in light of the fact that defects in MMR have been associated with skin cancers found in the HNPCC variant Muir–Torre syndrome. Furthermore, we searched for both FANCI and MMR mutations within sequenced melanoma genomes using cBioPortal (51, 52) and the Catalogue of Somatic Mutations in Cancer database (53). We identified mutations in *FANCI*, *MSH2*, *MSH6*, *MLH1*, and *PMS2* (Supplementary Fig. S7A–S7F). The majority of *FANCI* mutations target the helicase domain, including domains important for enzyme function, such as the Fe–S domain and helicase boxes III to V (Supplementary Fig. S7A; ref. 54). In addition, some of the mutations have been detected previously. The FANCI^{P47} residue was targeted in breast cancer and was shown to be ATPase and helicase inactive *in vitro* (39). The splice mutant FANCI^{R831} is an allele in Fanconi anemia and eliminates conserved helicase boxes required for enzyme function (39, 54, 55). To determine if loss of FANCI ATPase/helicase/translocase activity disrupts the UV response, we attempted to express the catalytic inactive FANCI^{K52R} mutant in FA-J cells. Because FANCI-deficient FA-J cells are defective in the UV response and the FANCI^{K52R}

mutant has weak expression compared with FANCI^{WT}, it was unclear if the mutant was defective in complementing FA-J cells or mediating the UV response. Thus, we overexpressed the FANCI^{K52R} mutant in U2OS cells. Here, we found significant defects in lesion clearance at 16 hours following UV damage, but no significant affect on RPA phosphorylation at this time point (Supplementary Fig. S8A–S8C). Thus, loss of FANCI expression could disrupt checkpoint activation, whereas expression of an enzyme inactive mutant could dominantly disrupt repair.

Further supporting that multiple pathways contribute to high-fidelity repair after UV irradiation, similar to skin tumors from XP patients (56), MMR- and FANCI-deficient cells display an elevated frequency of UV-induced C > T point mutations (Supplementary Table S1; ref. 14). Similar to FANCI deficiency, MMR deficiency also has modest effects on UV sensitivity despite reduced checkpoint and apoptotic responses (12, 57). Thus, we propose that FANCI intersects MMR- and NER-dependent repair pathways to promote efficient checkpoint activation, lesion clearance, and suppress UV-induced mutations (Fig. 5G). Conceivably, in the absence of FANCI and its checkpoint function error-prone polymerases induce mutations at sites of UV-induced lesions. Indeed, the high-fidelity TLS polymerase, pol η , has reduced foci formation in response to global UV irradiation in FANCI-deficient cells (Supplementary Fig. S9A–S9C). Correspondingly, MSH2-deficient cells have defective UV-induced PCNA mono-ubiquitination and TLS foci formation (58).

The NER factor XPA contributes to the S-phase checkpoint following UV-induced irradiation. However, not all NER factors are required, suggesting that this checkpoint function is distinct from NER repair in G₁ phase (4). Our findings further suggest that XPF promotes RPA phosphorylation in S-phase cells (Fig. 4A–C). Interestingly, XPF is the Fanconi anemia gene, FANCF (30). Given that XPF promotes FANCI accumulation in S-phase cells, our data also suggest that FANCI functions downstream of this Fanconi anemia factor to promote RPA phosphorylation throughout S-phase. NER-dependent incision may provide a better substrate or change the DNA structure, enabling distribution of FANCI at the lesion site (Fig. 5G). Here, FANCI could facilitate repair of lesions ahead of the replication fork through checkpoint induction and the arrest of DNA synthesis to limit mutation induction. Conceivably this function is shared by FANCI partners, such as Bloom's syndrome helicase (BLM), or the Fanconi anemia pathway, explaining its link to the UV response and checkpoints that limit genomic instability (59-62). It has been long proposed that ATR-BLM and Fanconi anemia pathway interactions maintain genomic stability by restoring productive replication following replication stress (63-65).

The 2-step mobilization of FANCI to UV-induced lesions, localization by MMR and further accumulation after NER-dependent postincision could ensure pathway coordination. Indeed, the combined loss of NER and MMR enhances UV-induced mutagenesis (10). Although MMR and NER proteins have been shown to have overlapping substrates (66), it remains to be determined whether they bind the same or a distinct type of UV lesion. FANCI loading by MLH1 would be reminiscent of the requirement of the bacterial MutL, homologous to the MutL α complex, for loading helicase II (UvrD) onto DNA (67). Helicase II functions with DNA polymerase I to release oligonucleotide fragments containing UV photoproducts (68). In contrast to Helicase II, our data do not support a role for FANCI or MMR in gap repair

(Figs. 4A, B, and F–H and Supplementary Fig. S4D and S4E). However, these findings do not exclude the possibility that MMR and FANCI contribute to the fidelity of NER-dependent gap filling. Alternatively, loading of FANCI by MMR factors could unwind and disrupt secondary DNA structures that impede NER processing. Indeed, MMR factors bind secondary structures such as G-4 quadruplex DNA that FANCI unwinds (69, 70). FANCI also depends on MLH1 for localization to sites of DNA interstrand crosslinks (29).

Collectively, the data presented in this manuscript provide a framework for understanding the contributions of distinct DNA repair pathways to the DNA damage response to UV irradiation in human cells. The identification of a novel function for MMR in localizing FANCI to sites of UV-induced damage could be useful for several reasons. First, it could help in the discrimination between missense and pathogenic MMR variants. Loss of FANCI localization and function could be uniquely disrupted by MMR gene mutations as found in tumors in which canonical MMR is intact. Second, the MMR-FANCI pathway could represent a unique tumor suppression pathway that provides opportunities for selective therapy in effected tumors. In melanoma, loss of FANCI function or expression could be a consequence of not only FANCI mutations (Supplementary Fig. S7A), but also MMR mutations. Indeed, ~5.7% of tumors are affected by FANCI mutations, which did not co-segregate with MMR gene mutations (51, 52). Associated skin tumors may be selectively sensitive to interstrand crosslink-inducing agents, which is a hallmark of FA-J patient cells. In light of the recent finding that XPF is the Fanconi anemia gene, FANCD1 (30), it will be important to determine if the Fanconi anemia pathway has a more fundamental role in the response to UV irradiation and/or in reducing the emergence of disease.

Supplementary Material

Refer to Web version on PubMed Central for supplementary material.

Acknowledgments

The authors thank Dr. C. Heinen (University of Connecticut Health Center) for comments on the manuscript, Dr. J. Hays (Oregon State University) for helpful discussions, and B. Morehouse, C. Brown, and N. Patil for technical assistance and quantification of experiments.

Grant Support

This work was supported by the NIH (RO1 CA129514-01A1) and charitable contributions from Mr. and Mrs. E.T. Vitone Jr.

References

1. Cleaver JE. Defective repair replication of DNA in xeroderma pigmentosum. *Nature*. 1968; 218:652–6. [PubMed: 5655953]
2. Hoeijmakers JH. Genome maintenance mechanisms for preventing cancer. *Nature*. 2001; 411:366–74. [PubMed: 11357144]
3. Gillet LCJ, Schärer OD. Molecular mechanisms of mammalian global genome nucleotide excision repair. *Chem Rev*. 2006; 106:253–76. [PubMed: 16464005]
4. Bomgardner RD, Lupardus PJ, Soni DV, Yee MC, Ford JM, Cimprich KA. Opposing effects of the UV lesion repair protein XPA and UV bypass polymerase eta on ATR checkpoint signaling. *EMBO J*. 2006; 25:2605–14. [PubMed: 16675950]

5. Gilljam KM, Muller R, Liabakk NB, Otterlei M. Nucleotide excision repair is associated with the replisome and its efficiency depends on a direct interaction between XPA and PCNA. *PLoS ONE*. 2012; 7:e49199. [PubMed: 23152873]
6. Sogo JM, Lopes M, Foiani M. Fork reversal and ssDNA accumulation at stalled replication forks owing to checkpoint defects. *Science*. 2002; 297:599–602. [PubMed: 12142537]
7. Byun TS, Pacek M, Yee M-C, Walter JC, Cimprich KA. Functional uncoupling of MCM helicase and DNA polymerase activities activates the ATR-dependent checkpoint. *Genes Dev*. 2005; 19:1040–52. [PubMed: 15833913]
8. Cortez D. Unwind and slow down: checkpoint activation by helicase and polymerase uncoupling. *Genes Dev*. 2005; 19:1007–12. [PubMed: 15879550]
9. Pathania S, Nguyen J, Hill SJ, Scully R, Adelmant GO, Marto JA, et al. BRCA1 is required for postreplication repair after UV-induced DNA damage. *Mol Cell*. 2011; 44:235–51. [PubMed: 21963239]
10. Nara K, Nagashima F, Yasui A. Highly elevated ultraviolet-induced mutation frequency in isolated Chinese hamster cell lines defective in nucleotide excision repair and mismatch repair proteins. *Cancer Res*. 2001; 61:50–2. [PubMed: 11196196]
11. Meira LB, Cheo DL, Reis AM, Claij N, Burns DK, te Riele H, et al. Mice defective in the mismatch repair gene Msh2 show increased predisposition to UVB radiation-induced skin cancer. *DNA Repair*. 2002; 1:929–34. [PubMed: 12531020]
12. Yoshino M, Nakatsu Y, te Riele H, Hirota S, Kitamura Y, Tanaka K. Additive roles of XPA and MSH2 genes in UVB-induced skin tumorigenesis in mice. *DNA Repair*. 2002; 1:935–40. [PubMed: 12531021]
13. Seifert M, Scherer SJ, Edelmann W, Bohm M, Meineke V, Lobrich M, et al. The DNA-mismatch repair enzyme hMSH2 modulates UV-B-induced cell cycle arrest and apoptosis in melanoma cells. *J Invest Dermatol*. 2008; 128:203–13. [PubMed: 17611581]
14. Borgdorff V, Pauw B, van Hees-Stuivenberg S, de Wind N. DNA mismatch repair mediates protection from mutagenesis induced by short-wave ultraviolet light. *DNA Repair*. 2006; 5:1364–72. [PubMed: 16880010]
15. Kunkel TA, Erie DA. DNA mismatch repair. *Annu Rev Biochem*. 2005; 74:681–710. [PubMed: 15952900]
16. Jiricny J. The multifaceted mismatch-repair system. *Nat Rev Mol Cell Biol*. 2006; 7:335–46. [PubMed: 16612326]
17. Kaina B, Christmann M, Naumann S, Roos WP. MGMT: key node in the battle against genotoxicity, carcinogenicity and apoptosis induced by alkylating agents. *DNA Repair (Amst)*. 2007; 6:1079–99. [PubMed: 17485253]
18. Mu D, Tursun M, Duckett DR, Drummond JT, Modrich P, Sancar A. Recognition and repair of compound DNA lesions (base damage and mismatch) by human mismatch repair and excision repair systems. *Mol Cell Biol*. 1997; 17:760–9. [PubMed: 9001230]
19. Wang H, Lawrence CW, Li GM, Hays JB. Specific binding of human MSH2.MSH6 mismatch-repair protein heterodimers to DNA incorporating thymine- or uracil-containing UV light photoproducts opposite mismatched bases. *J Biol Chem*. 1999; 274:16894–900. [PubMed: 10358035]
20. Mathiak M, Rutten A, Mangold E, Fischer H-P, Ruzicka T, Friedl W, et al. Loss of DNA mismatch repair proteins in skin tumors from patients with Muir-Torre syndrome and MSH2 or MLH1 germline mutations: establishment of immunohistochemical analysis as a screening test. *Am J Surg Pathol*. 2002; 26:338–43. [PubMed: 11859205]
21. Kruse R, Rutten A, Lamberti C, Hosseiny-Malayeri HR, Wang Y, Ruelfs C, et al. Muir-Torre phenotype has a frequency of DNA mismatch-repair-gene mutations similar to that in hereditary nonpolyposis colorectal cancer families defined by the Amsterdam criteria. *Am J Hum Genet*. 1998; 63:63–70. [PubMed: 9634524]
22. Suspiro A, Fidalgo P, Cravo M, Albuquerque C, Ramalho E, Leitao CN, et al. The Muir-Torre syndrome: a rare variant of hereditary nonpolyposis colorectal cancer associated with hMSH2 mutation. *Am J Gastroenterol*. 1998; 93:1572–4. [PubMed: 9732950]

23. Cantor SB, Bell DW, Ganesan S, Kass EM, Drapkin R, Grossman S, et al. BACH1, a novel helicase-like protein, interacts directly with BRCA1 and contributes to its DNA repair function. *Cell*. 2001; 105:149–60. [PubMed: 11301010]
24. Peng M, Litman R, Xie J, Sharma S, Brosh RM Jr, Cantor SB. The FANCI/MutL α interaction is required for correction of the cross-link response in FA-J cells. *EMBO J*. 2007; 26:3238–49. [PubMed: 17581638]
25. Gong Z, Kim JE, Leung CC, Glover JN, Chen J. BACH1/FANCI acts with TopBP1 and participates early in DNA replication checkpoint control. *Mol Cell*. 2010; 37:438–46. [PubMed: 20159562]
26. Cotta-Ramusino C, McDonald ER 3rd, Hurov K, Sowa ME, Harper JW, Elledge SJ. A DNA damage response screen identifies RHINO, a 9-1-1 and TopBP1 interacting protein required for ATR signaling. *Science*. 2011; 332:1313–7. [PubMed: 21659603]
27. Xie J, Peng M, Guillemette S, Quan S, Maniatis S, Wu Y, et al. FANCI/BACH1 acetylation at lysine 1249 regulates the DNA damage response. *PLoS Genet*. 2012; 8:e1002786. [PubMed: 22792074]
28. Xie J, Litman R, Wang S, Peng M, Guillemette S, Rooney T, et al. Targeting the FANCI-BRCA1 interaction promotes a switch from recombination to pol η -dependent bypass. *Oncogene*. 2010; 29:2499–508. [PubMed: 20173781]
29. Suhasini AN, Sommers JA, Muniandy PA, Coulombe Y, Cantor SB, Masson JY, et al. Fanconi anemia group J helicase MRE11 nuclease interact to facilitate the DNA damage response. *Mol Cell Biol*. 2013; 33:2212–27. [PubMed: 23530059]
30. Bogliolo M, Schuster B, Stoepker C, Derkunt B, Su Y, Raams A, et al. Mutations in ERCC4, encoding the DNA-repair endonuclease XPF, cause Fanconi anemia. *Am J Hum Genet*. 2013; 92:800–6. [PubMed: 23623386]
31. Kashiyama K, Nakazawa Y, Pilz DT, Guo C, Shimada M, Sasaki K, et al. Malfunction of nuclease ERCC1-XPF results in diverse clinical manifestations and causes cockayne syndrome, xeroderma pigmentosum, and fanconi anemia. *Am J Hum Genet*. 2013; 92:807–19. [PubMed: 23623389]
32. Nakatani Y, Ogryzko V. Immunoaffinity purification of mammalian protein complexes. *Methods Enzymol*. 2003; 370:430–44. [PubMed: 14712665]
33. Kannouche P, Broughton BC, Volker M, Hanaoka F, Mullenders LH, Lehmann AR. Domain structure, localization, and function of DNA polymerase η , defective in xeroderma pigmentosum variant cells. *Genes Dev*. 2001; 15:158–72. [PubMed: 11157773]
34. Watanabe K, Tateishi S, Kawasuji M, Tsurimoto T, Inoue H, Yamaizumi M. Rad18 guides pol η to replication stalling sites through physical interaction and PCNA monoubiquitination. *EMBO J*. 2004; 23:3886–96. [PubMed: 15359278]
35. Mone MJ, Volker M, Nikaido O, Mullenders LH, van Zeeland AA, Verschure PJ, et al. Local UV-induced DNA damage in cell nuclei results in local transcription inhibition. *EMBO Rep*. 2001; 2:1013–7. [PubMed: 11713193]
36. Chiu RK, Brun J, Ramaekers C, Theys J, Weng L, Lambin P, et al. Lysine 63-polyubiquitination guards against translesion synthesis-induced mutations. *PLoS Genet*. 2006; 2:e116. [PubMed: 16789823]
37. Limsirichaikul S, Niimi A, Fawcett H, Lehmann A, Yamashita S, Ogi T. A rapid non-radioactive technique for measurement of repair synthesis in primary human fibroblasts by incorporation of ethynyl deoxyuridine (EdU). *Nucleic Acids Res*. 2009; 37:e31. [PubMed: 19179371]
38. Hidaka M, Takagi Y, Takano TY, Sekiguchi M. PCNA-MutS α -mediated binding of MutL α to replicative DNA with mismatched bases to induce apoptosis in human cells. *Nucleic Acids Res*. 2005; 33:5703–12. [PubMed: 16204460]
39. Cantor S, Drapkin R, Zhang F, Lin Y, Han J, Pamidi S, et al. The BRCA1-associated protein BACH1 is a DNA helicase targeted by clinically relevant inactivating mutations. *Proc Natl Acad Sci U S A*. 2004; 101:2357–62. [PubMed: 14983014]
40. Volker M, Mone MJ, Karmakar P, van Hoffen A, Schul W, Vermeulen W, et al. Sequential assembly of the nucleotide excision repair factors *in vivo*. *Mol Cell*. 2001; 8:213–24. [PubMed: 11511374]

41. Staresinic L, Fagbemi AF, Enzlin JH, Gourdin AM, Wijgers N, Dunand-Sauthier I, et al. Coordination of dual incision and repair synthesis in human nucleotide excision repair. *EMBO J*. 2009; 28:1111–20. [PubMed: 19279666]
42. Sertic S, Pizzi S, Cloney R, Lehmann AR, Marini F, Plevani P, et al. Human exonuclease 1 connects nucleotide excision repair (NER) processing with checkpoint activation in response to UV irradiation. *Proc Natl Acad Sci U S A*. 2011; 108:1, 3647–52.
43. Young LC, Hays JB, Tron VA, Andrew SE. DNA mismatch repair proteins: potential guardians against genomic instability and tumorigenesis induced by ultraviolet photoproducts. *J Invest Dermatol*. 2003; 121:435–40. [PubMed: 12925197]
44. Greenberg RA, Sobhian B, Pathania S, Cantor SB, Nakatani Y, Livingston DM. Multifactorial contributions to an acute DNA damage response by BRCA1/BARD1-containing complexes. *Genes Dev*. 2006; 20:34–46. [PubMed: 16391231]
45. Yu X, Chini CC, He M, Mer G, Chen J. The BRCT domain is a phospho-protein binding domain. *Science*. 2003; 302:639–42. [PubMed: 14576433]
46. Kaufmann WK. The human intra-S checkpoint response to UVC-induced DNA damage. *Carcinogenesis*. 2010; 31:751–65. [PubMed: 19793801]
47. Carty MP, Zernik-Kobak M, McGrath S, Dixon K. UV light-induced DNA synthesis arrest in HeLa cells is associated with changes in phosphorylation of human single-stranded DNA-binding protein. *EMBO J*. 1994; 13:2114–23. [PubMed: 8187764]
48. Niu H, Erdjument-Bromage H, Pan ZQ, Lee SH, Tempst P, Hurwitz J. Mapping of amino acid residues in the p34 subunit of human single-stranded DNA-binding protein phosphorylated by DNA-dependent protein kinase and Cdc2 kinase *in vitro*. *J Biol Chem*. 1997; 272:12634–41. [PubMed: 9139719]
49. Zernik-Kobak M, Vasunia K, Connelly M, Anderson CW, Dixon K. Sites of UV-induced phosphorylation of the p34 subunit of replication protein A from HeLa cells. *J Biol Chem*. 1997; 272:23896–904. [PubMed: 9295339]
50. Auclair Y, Rouget R, Affar el B, Drobetsky EA. ATR kinase is required for global genomic nucleotide excision repair exclusively during S phase in human cells. *Proc Natl Acad Sci U S A*. 2008; 105:17896–901. [PubMed: 19004803]
51. Cerami E, Gao J, Dogrusoz U, Gross BE, Sumer SO, Aksoy BA, et al. The cBio cancer genomics portal: an open platform for exploring multidimensional cancer genomics data. *Cancer Discov*. 2012; 2:401–4. [PubMed: 22588877]
52. Gao J, Aksoy BA, Dogrusoz U, Dresdner G, Gross B, Sumer SO, et al. Integrative analysis of complex cancer genomics and clinical profiles using the cBioPortal. *Sci Signal*. 2013; 6:p11.
53. Forbes SA, Bindal N, Bamford S, Cole C, Kok CY, Beare D, et al. COSMIC: mining complete cancer genomes in the Catalogue of Somatic Mutations in Cancer. *Nucleic Acids Res*. 2011; 39:D945–50. [PubMed: 20952405]
54. Cantor SB, Guillemette S. Hereditary breast cancer and the BRCA1-associated FANCD1/BACH1/BRIP1. *Future Oncol*. 2011; 7:253–61. [PubMed: 21345144]
55. Gupta R, Sharma S, Sommers JA, Jin Z, Cantor SB, Brosh RM Jr. Analysis of the DNA substrate specificity of the human BACH1 helicase associated with breast cancer. *J Biol Chem*. 2005; 280:25450–60. [PubMed: 15878853]
56. Dumaz N, Drougard C, Sarasin A, Daya-Grosjean L. Specific UV-induced mutation spectrum in the p53 gene of skin tumors from DNA-repair-deficient xeroderma pigmentosum patients. *Proc Natl Acad Sci U S A*. 1993; 90:10529–33. [PubMed: 8248141]
57. van Oosten M, Stout GJ, Backendorf C, Rebel H, de Wind N, Darroudi F, et al. Mismatch repair protein Msh2 contributes to UVB-induced cell cycle arrest in epidermal and cultured mouse keratinocytes. *DNA Repair*. 2005; 4:81–9. [PubMed: 15533840]
58. Lv L, Wang F, Ma X, Yang Y, Wang Z, Liu HL, et al. Mismatch repair protein MSH2 regulates translesion DNA synthesis following exposure of cells to UV radiation. *Nucleic Acids Res*. 2013 Sep 12. [Epub ahead of print].
59. Suhasini AN, Rawtani NA, Wu Y, Sommer JA, Sharma S, Mosedale G, et al. Interaction between the helicases genetically linked to Fanconi anemia group J and Bloom's syndrome. *EMBO J*. 2011; 30:692–705. [PubMed: 21240188]

60. Kelsall IR, Langenick J, MacKay C, Patel KJ, Alpi AF. The Fanconi anaemia components UBE2T and FANCM are functionally linked to nucleotide excision repair. *PLoS ONE*. 2012; 7:e36970. [PubMed: 22615860]
61. Singh TR, Bakker ST, Agarwal S, Jansen M, Grassman E, Godthelp BC, et al. Impaired FANCD2 monoubiquitination and hypersensitivity to camptothecin uniquely characterize Fanconi anemia complementation group M. *Blood*. 2009; 114:174–80. [PubMed: 19423727]
62. Nalepa G, Enzor R, Sun Z, Marchal C, Park SJ, Yang Y, et al. Fanconi anemia signaling network regulates the spindle assembly checkpoint. *J Clin Invest*. 2013; 123:3839–47. [PubMed: 23934222]
63. Davies SL, North PS, Dart A, Lakin ND, Hickson ID. Phosphorylation of the Bloom's syndrome helicase and its role in recovery from S-phase arrest. *Mol Cell Biol*. 2004; 24:1279–91. [PubMed: 14729972]
64. Olson E, Nievera CJ, Klimovich V, Fanning E, Wu X. RPA2 is a direct downstream target for ATR to regulate the S-phase checkpoint. *J Biol Chem*. 2006; 281:39517–33. [PubMed: 17035231]
65. Sobek A, Stone S, Costanzo V, de Graaf B, Reuter T, de Winter J, et al. Fanconi anemia proteins are required to prevent accumulation of replication-associated DNA double-strand breaks. *Mol Cell Biol*. 2006; 26:425–37. [PubMed: 16382135]
66. Zhao J, Jain A, Iyer RR, Modrich PL, Vasquez KM. Mismatch repair and nucleotide excision repair proteins cooperate in the recognition of DNA interstrand crosslinks. *Nucleic Acids Res*. 2009; 37:4420–9. [PubMed: 19468048]
67. Mechanic LE, Frankel BA, Matson SW. *Escherichia coli* MutL loads DNA helicase II onto DNA. *J Biol Chem*. 2000; 275:38337–46. [PubMed: 10984488]
68. Caron PR, Kushner SR, Grossman L. Involvement of helicase II (UvrD gene product) and DNA polymerase I in excision mediated by the uvrABC protein complex. *Proc Natl Acad Sci U S A*. 1985; 82:4925–9. [PubMed: 3161077]
69. Larson ED, Duquette ML, Cummings WJ, Streiff RJ, Maizels N. MutSa binds to and promotes synapsis of transcriptionally activated immunoglobulin switch regions. *Curr Biol*. 2005; 15:470–4. [PubMed: 15753043]
70. Wu Y, Shin-Ya K, Brosh RM Jr. FANCI helicase defective in Fanconi anemia and breast cancer unwinds g-quadruplex DNA to defend genomic stability. *Mol Cell Biol*. 2008; 28:4116–28. [PubMed: 18426915]

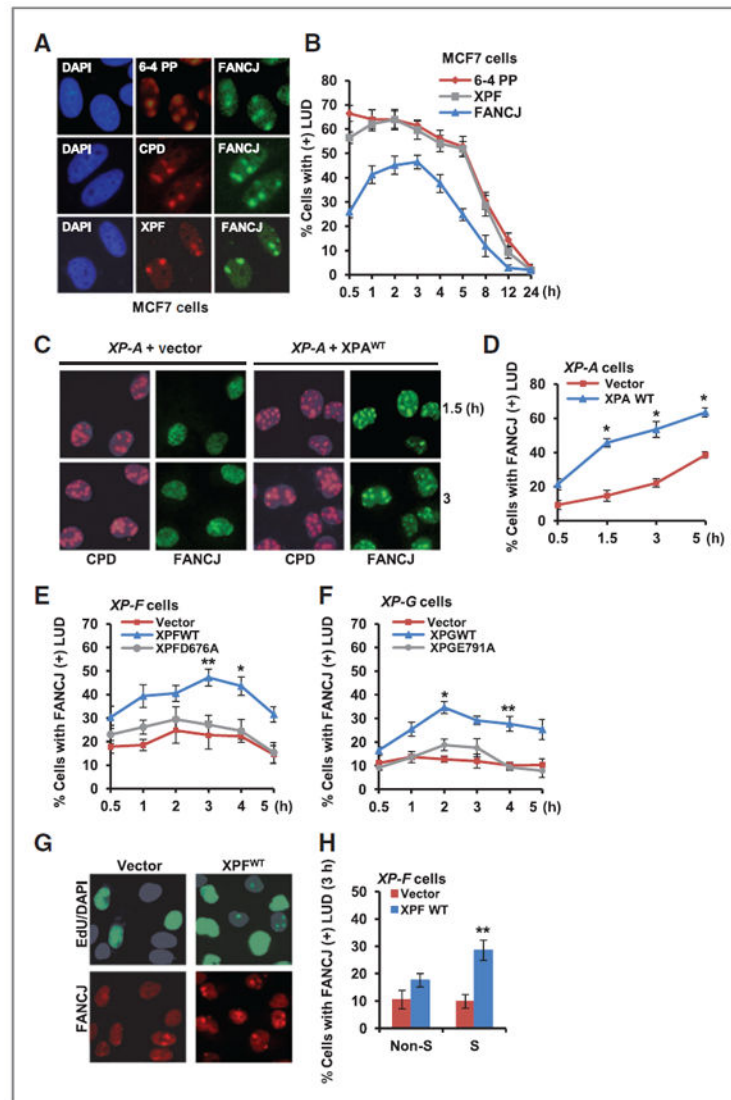


Figure 1.

FANCJ recruitment to sites of LUDs is dependent on NER dual incision and is predominantly in S phase. A, MCF7 cells were UV irradiated through 5- μ m micropore filters to generate LUDs and co-immunostained with the indicated Abs. Representative images are shown 1 hour after UV irradiation. B, quantification of MCF7 cells positive for FANCJ, XPF, or 6-4 PP LUDs. C, *XP-A* cells complemented with empty vector or *XPA*^{WT} were UV irradiated through 3- μ m micropore filters to generate LUDs and co-immunostained with the indicated Abs. D, quantification of *XP-A* cells with FANCJ-positive LUDs. E, *XP-F* cells complemented with empty vector, *XPF*^{WT}, or *XPF*^{D676A} were treated as in C and FANCJ-positive LUDs were quantified. F, *XP-G* cells complemented with empty vector, *XPG*^{WT}, or *XPG*^{E791A} were treated as in C and FANCJ-positive LUDs were quantified. G, *XP-F* cells complemented with empty vector or *XPF*^{WT} were UV irradiated through 5- μ m micropore filters, incubated with EdU, and co-immunostained with the indicated Abs. H, quantification of *XP-F* cells with FANCJ-positive LUDs. Where shown, error bars represent

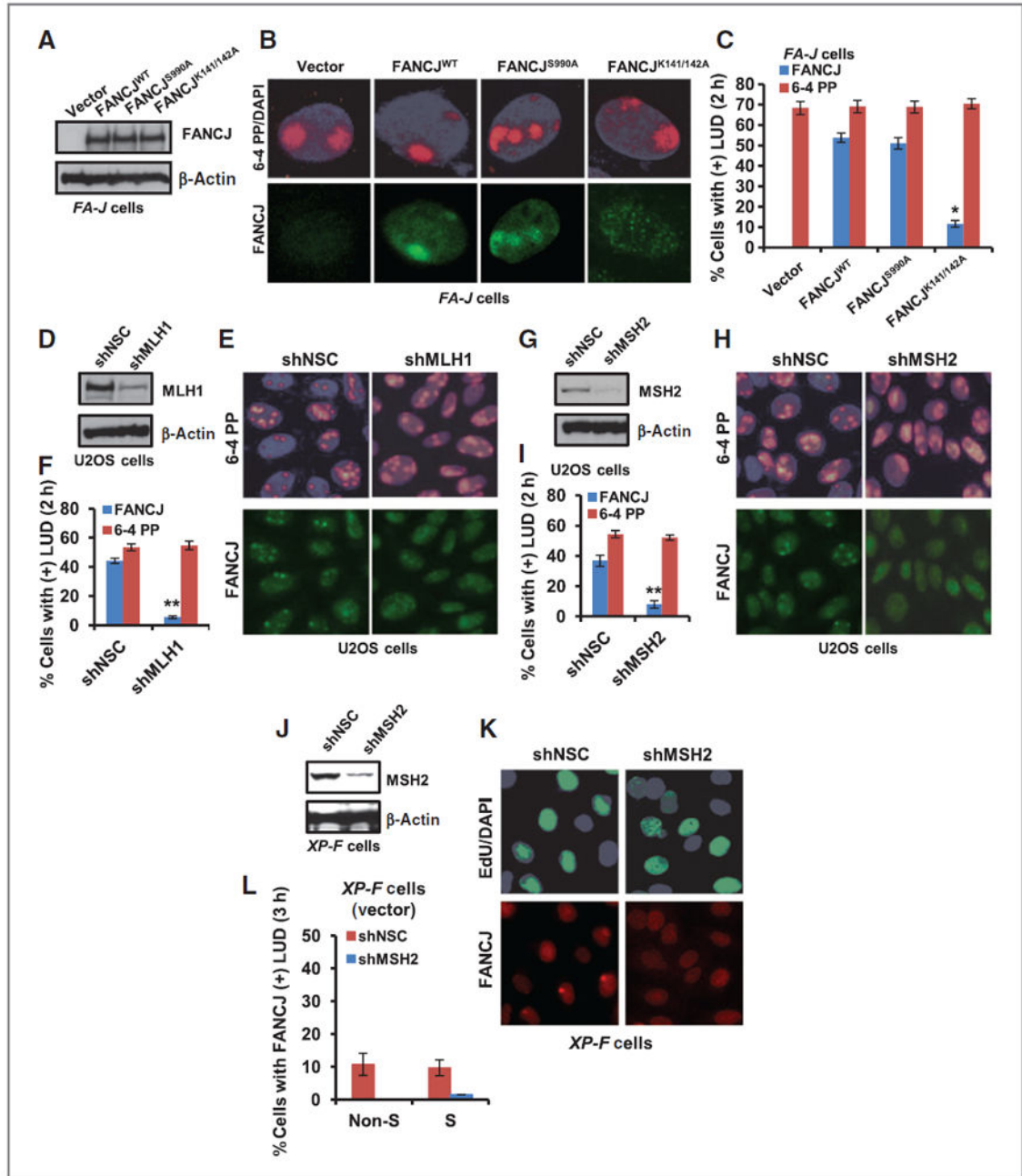
the standard deviation of the mean of 3 independent experiments, asterisks denote Significance from Student 2-tailed, unpaired *t* test: *, *P* 0.05; **, *P* 0.01; ***, *P* 0.005.

Author Manuscript

Author Manuscript

Author Manuscript

Author Manuscript

**Figure 2.**

FANCD1 recruitment to sites of LUDs is MMR dependent. **A**, FA-J cells were complemented with empty vector, FANCD1^{WT}, FANCD1^{S990A}, or FANCD1^{K141/142A} and analyzed by immunoblot. **B** and **C**, FA-J cells were UV irradiated through 5- μ m micropore membrane filters, coimmunostained with the indicated Abs (**B**), and quantified for FA-J cells with FANCD1- and 6-4 PP-positive LUDs (**C**). **D–F**, U2OS cells containing shRNA vectors targeting MLH1 or NSC were analyzed by immunoblot (**D**) and UV irradiated through micropore filters (**E**) and quantified for cells with FANCD1- or 6-4 PP-positive LUDs (**F**). **G–I**, U2OS cells containing shRNA vectors targeting MSH2 or NSC were analyzed by

immunoblot (G) and UV irradiated through micropore filters (H) and quantified for cells with FANCI- or 6-4 PP-positive LUDs (I). J, *XP-F* cells complemented with empty vector were stably depleted of MSH2 versus NSC and analyzed by immunoblot. K, cells were treated as in E and processed for EdU incorporation and coimmunostained with the indicated Abs and quantified for cells with FANCI-positive LUDs (L). Error bars represent the standard deviation of the mean of three independent experiments.

Author Manuscript

Author Manuscript

Author Manuscript

Author Manuscript

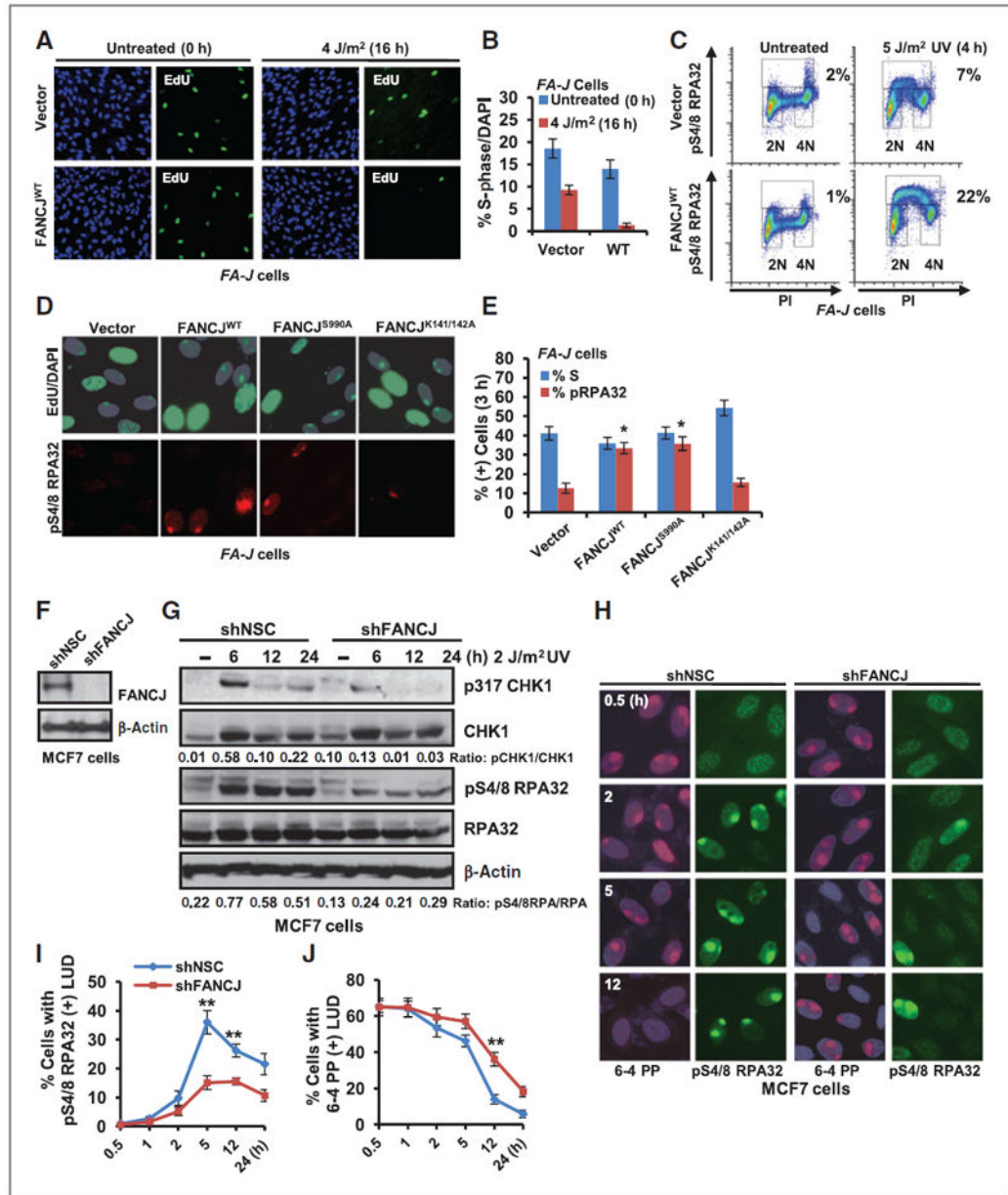


Figure 3.

FANCJ contributes to the UV-induced checkpoint response. **A**, *FA-J* cells complemented with empty vector or FANCJ^{WT} were left untreated and pulsed for 45 minutes with 10 μmol/L EdU or globally UV irradiated and pulsed for 45 minutes with 10 μmol/L EdU 16 hours later. Cells were processed for EdU incorporation and costained with DAPI. **B**, quantification of EdU incorporation/total number of DAPI (+) cells. 1,000 DAPI cells were quantified for each experiment in triplicate. **C**, *FA-J* cells complemented with empty vector or FANCJ^{WT} were left untreated or UV irradiated and analyzed by FACS sorting for phospho-S4/8 RPA32–positive cells; representative plots are shown. **D**, *FA-J* cells were UV irradiated through 5-μm micropore filters, incubated with 10 μmol/L EdU for 3 hours, and coimmunostained with phospho-S4/8 RPA32 Ab. **E**, quantification of phospho-S4/8 RPA32–

positive LUDs in S-phase cells. F and G, MCF7 cells containing shRNA vectors targeting FANCI or NSC were analyzed by immunoblot with the indicated Abs (F) or at the indicated time points after UV irradiation (G). The ratio of phospho-protein/total protein by densitometry using Image J software is quantified. H, the MCF7 cells shown were UV irradiated through 5- μ m filters to generate LUDs and coimmunostained with the indicated Abs at several time points. I, quantification of cells with phospho-S4/8 RPA32-positive LUDs. J, quantification of 6-4 PP-positive LUDs. Where shown, error bars represent the standard deviation of the mean of three independent experiments.

Author Manuscript

Author Manuscript

Author Manuscript

Author Manuscript

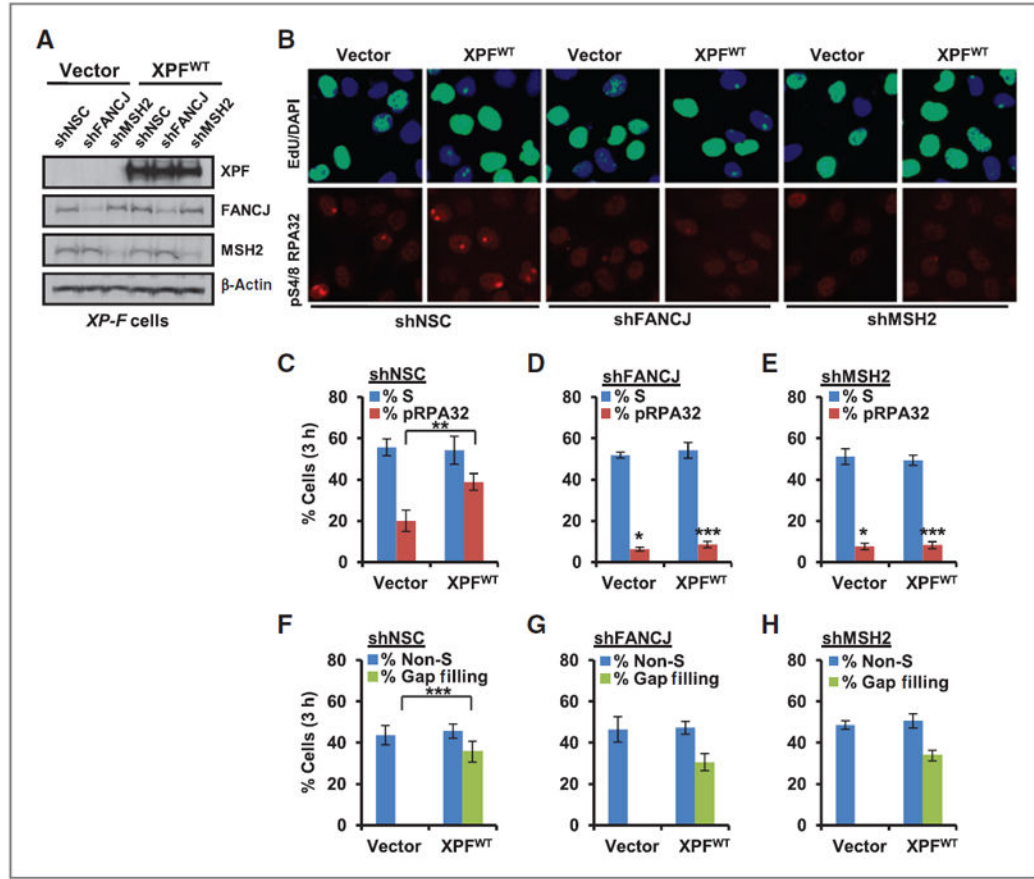
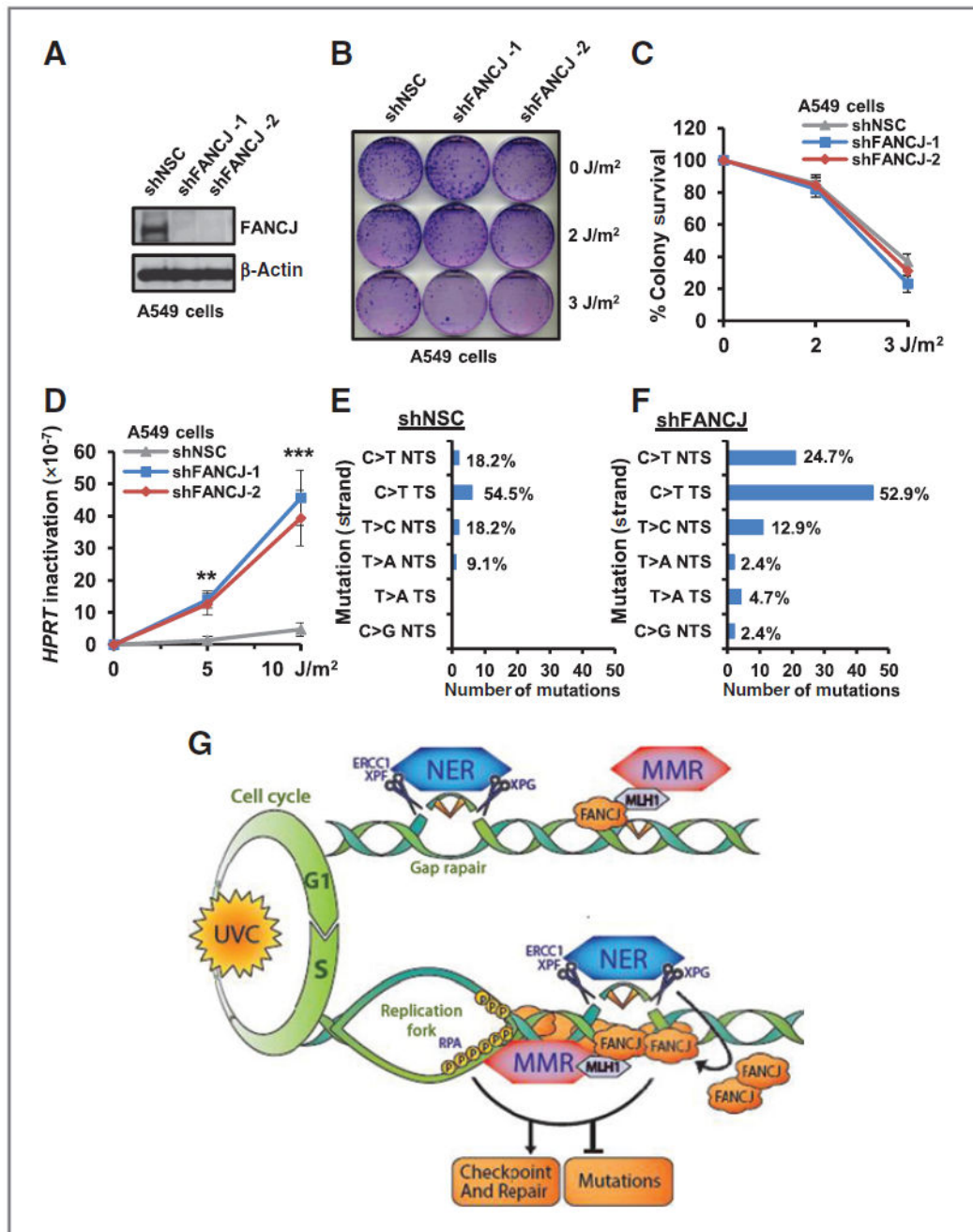


Figure 4.

FANCI and MSH2 are required for NER-dependent and -independent induction of RPA phosphorylation in S phase, but not for gap repair. A, *XP-F* cells complemented with empty vector or XPF^{WT} were stably depleted of FANCI, MSH2, or NSC using shRNA vectors and analyzed by immunoblot. B, cells were UV irradiated through 5- μ m micropore filters, incubated with EdU, and coimmunostained with the indicated Abs 3 hours after treatment. C–E, quantification of phospho-S4/8 RPA32–positive LUDs in S-phase cells expressing shNSC (C), shFANCI (D), and shMSH2 (E). F–H, quantification of NER-dependent gap filling in non-S-phase cells expressing shNSC (F), shFANCI (G), and shMSH2 (H). Where shown, error bars represent the standard deviation of the mean of three independent experiments.

**Figure 5.**

FANCI suppresses UV-induced mutations. A and B, A549 cells expressing individual shRNA vectors targeting FANCI or NSC were analyzed by immunoblot (A) and left untreated or globally UV irradiated and analyzed for colony survival (B). C, quantification of surviving colonies. D, quantification of 6-TG-resistant *HPRT* mutant colonies from mutagenesis assay. E and F, quantification of the distribution of *HPRT*-inactivating mutations in A549 cells expressing shRNA to NSC (E) and/or shRNAs to FANCI (combined; F). G, model of FANCI function in response to UV irradiation. NER and MMR

factors are recruited to sites of local UV-induced damage in non-S-phase cells where NER, but not MMR, is required for gap filling. In S-phase cells, both NER and MMR factors contribute to the accumulation of FANCD1. MMR through MLH1 binding localizes FANCD1 to sites of UV-induced damage. NER incision enhances the accumulation of FANCD1 at the lesion site. Collectively, these events ensure a robust checkpoint response to limit the replication of damaged DNA, induction of mutations, and cancer. Where shown, error bars represent the standard deviation of the mean of three independent experiments.

Author Manuscript

Author Manuscript

Author Manuscript

Author Manuscript